

Shot Noise of Spin-Decohering Transport in Spin-Orbit Coupled Nanostructures

Ralitsa L. Dragomirova and Branislav K. Nikolić

Department of Physics and Astronomy, University of Delaware, Newark, DE 19716-2570, USA

We generalize the scattering theory of quantum shot noise to include the full spin-density matrix of electrons injected from a spin-filtering or ferromagnetic electrode into a quantum-coherent nanosstructure governed by various spin-dependent interactions. This formalism yields the spin-resolved shot noise power for different experimental measurement setups—with ferromagnetic source and ferromagnetic or normal drain electrodes—whose evaluation for the diffusive multichannel quantum wires with the Rashba (SO) spin-orbit coupling shows how spin *decoherence* and *dephasing* lead to dramatic enhancement of current fluctuations (with Fano factor $F > 1/3$). However, these processes and the corresponding shot noise increase are suppressed in narrow wires, which offers an experimental tool to probe spin decoherence parameters in confined SO-coupled open systems.

PACS numbers: 72.70.+m, 72.25.-b, 71.70.Ej, 73.23.-b

Over the past two decades, the exploration of the shot noise accompanying charge flow through mesoscopic conductors has become a major tool for gathering information about microscopic mechanisms of transport and correlations between charges which cannot be extracted from traditional conductance measurement.¹ Such nonequilibrium time-dependent fluctuations arise due to discreetness of charge, persist down to zero temperature (in contrast to thermal fluctuations which vanish at $T = 0$), and require stochasticity induced by either quantum-mechanical² backscattering of electrons within a mesoscopic (i.e., smaller than the inelastic scattering length³) structure or by random injection processes (as in the textbook example of Schottky vacuum diode).

The zero-frequency shot noise power spectrum $S = 2FI$ of conventional unpolarized charge current with average value I in the two-terminal non-interacting conductors reaches its maximum Poisson value (with Fano factor $F = 1$) when transport is determined by uncorrelated stochastic processes. On the other hand, the Pauli exclusion principle correlates electron motion and suppress the shot noise $F < 1$ of non-interacting carriers, while electron-electron interactions can also lead to super-Poissonian $F > 1$ noise signatures.¹ For example, the famous $F = 1/3$ universal suppression factor^{1,3} for non-interacting quasiparticles in two-terminal diffusive conductors is determined by the interplay of randomness in quantum-mechanical impurity scattering and the Pauli blocking imposed by their Fermi statistics.

In contrast to the wealth of information acquired on the shot noise in spin-degenerate transport, it is only recently that the study of spin-dependent shot noise in ferromagnetic-normal systems,⁴ where (usually assumed half-metallic) ferromagnetic source injects fully spin-polarized charge current into a normal region with interactions affect the spin of transported electron, has been initiated in two-terminal^{5,6,7} and multiterminal geometries.^{8,9} For example, it has been shown that spin-flip scattering can substantially increase the shot noise above $F = 1/3$ in diffusive wires attached to two ferromagnetic electrodes with antiparallel orientation of their magnetization,⁵ as well as in the setup with the ferromagnetic

source and a normal drain (collecting both spin species) electrodes. Thus, the enhanced shot noise power reveals additional sources of current fluctuation when spin degeneracy is lifted and particles from spin- \uparrow electron subsystem are converted into spin- \downarrow electrons. Microscopically, spin-flips are either instantaneous events generated by collision of electrons with magnetic impurities and spin-orbit (SO) dependent scattering off static disorder,⁷ or a continuous spin precession during electron free propagation⁶ in magnetic field imposed either externally or induced by the intrinsic SO couplings¹⁰ (whose “internal” magnetic field is momentum dependent).

At low temperatures, where small enough ($\lesssim 1 \mu\text{m}$) conductors become phase-coherent and Pauli blocking renders regular injection and collection of charge carriers from the bulk electrodes, the scattering theory of quantum transport provides^{1,11} the Khlus-Lesovik formula for the shot noise power in terms of the transmission eigenvalues T_n , $S = (4e^3V/h) \sum_{n=1}^M T_n(1-T_n)$, where V is linear response (time-independent) bias voltage.¹ This celebrated formula has transparent physical interpretation—in the basis of eigenchannels, which diagonalize $\mathbf{t}\mathbf{t}^\dagger$ with \mathbf{t} being the Landauer-Büttiker transmission matrix, a mesoscopic structure can be viewed as a parallel circuit of M (= number of transverse propagating orbital wave functions in the leads) independent one-dimensional conductors, each characterized by the transmission probability T_n . To get the shot noise through disordered systems, the Khlus-Lesovik formula has to be averaged¹ over a proper distribution of T_n . However, this standard route becomes *inapplicable* for spin-polarized injection where one has to take into account the *spin-density matrix* of injected electrons,¹² and therefore perform the calculations in the basis of transverse propagating modes (i.e., original orbital “conducting channels” which define the \mathbf{t} -matrix) of the source electrode.⁶

In this Rapid Communication we derive a generalization of the scattering matrix-based formulas for the shot noise to include both the “direction” of injected spins and the degree of their quantum coherence, as encoded into the spin polarization vector \mathbf{P} which specifies the spin density matrix of the current of quantum-transported

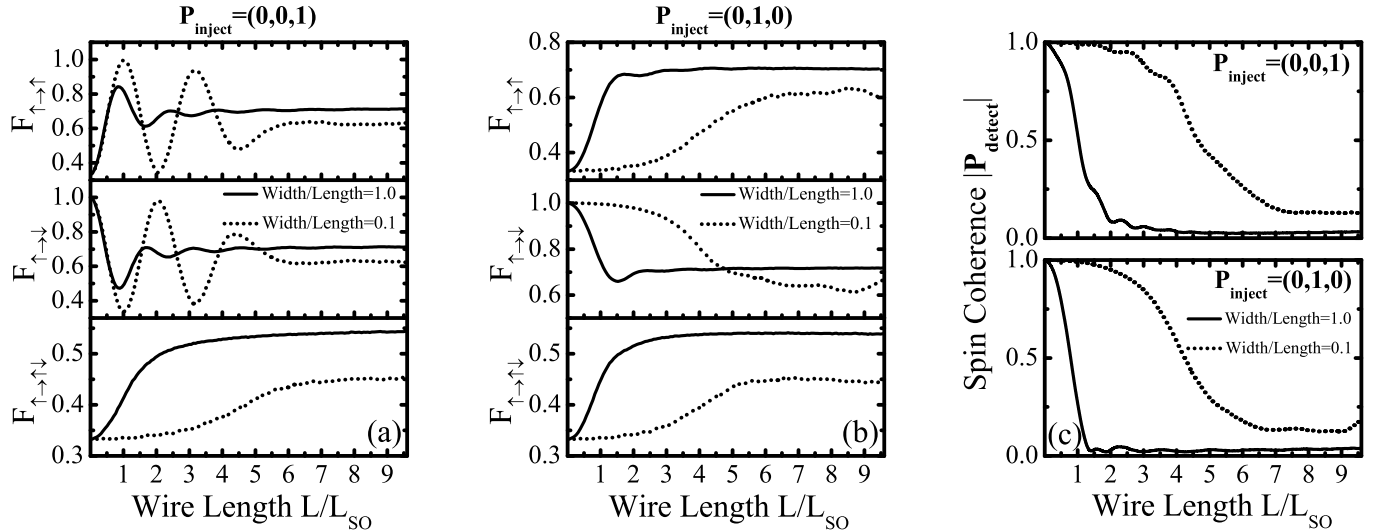


FIG. 1: (a) and (b): Fano factor vs the spin precession length L_{SO} for different two-probe measuring setups where fully spin- \uparrow polarized charge current is injected from the source into a diffusive Rashba SO coupled wire and spin-resolved charge currents I^{\uparrow} (top), I^{\downarrow} (middle), or both $I^{\uparrow} + I^{\downarrow}$ (bottom), are collected in the drain. Panel (c) shows the corresponding decay of the degree of phase-coherence of transported spin, as quantified by the magnitude of the Bloch vector of charge current,¹² which is $|\mathbf{P}_{\text{inject}}| = 1$ (signifying fully coherent pure spin state) in the left lead and pointing along the z -axis in (a) and the y -axis in (b).

electrons¹² $\hat{\rho}_c = (1 + \mathbf{P} \cdot \hat{\sigma})/2$. For example, in the case of quantum wires realized using a two-dimensional electron gas (2DEG) with the Rashba SO coupling¹⁰ (due to structural inversion asymmetry of the semiconductor heterostructure hosting the 2DEG in the xy -plane), which are described by the effective mass Hamiltonian

$$\hat{H} = \frac{\hat{p}_x^2 + \hat{p}_y^2}{2m^*} + \frac{\alpha}{\hbar} (\hat{p}_y \otimes \hat{\sigma}_x - \hat{p}_x \otimes \hat{\sigma}_y) + V_{\text{conf}}(y), \quad (1)$$

the internal momentum dependent magnetic field $\mathbf{B}(\mathbf{p}) = -(2\alpha/g\mu_B)(\hat{\mathbf{p}} \times \hat{z})$ (\hat{z} is the unit vector orthogonal to 2DEG) is nearly parallel to the transverse y -axis. Therefore, the injected z -axis polarized spins are precessing within the wires, while the y -axis polarized spins are in the eigenstates of the corresponding Zeeman term and do not precess while relaxing.¹² This leads to a difference in the shot noise when changing the spin-polarization vector of the injected current in the two-terminal “polarizer-analyzer” setups of Fig. 1(a) and 1(b).

Moreover, in both cases and within the asymptotic limit $L \gg L_{SO}$, where L is the wire length and L_{SO} is the spin precession length, we find the shot noise increase above the universal Fano factor $F = 1/3$ for all three measurement geometries: spin valves with (i) parallel [\uparrow -electrons injected from the left lead and \uparrow -electrons collected in the right lead], and (ii) antiparallel [\uparrow -electrons injected through a perfect Ohmic contact and \downarrow -electrons collected] magnetization of electrodes; as well as (iii) \uparrow -electrons injected with both \uparrow - and \downarrow -electrons being collected in the normal drain electrode. Note that on the $L_{SO} = \pi\hbar^2/(2m^*\alpha)$ scale spin precesses by an angle π (i.e., the state $|\uparrow\rangle$ evolves into

$|\downarrow\rangle$), which in weakly disordered¹² *bulk* systems also plays the role of characteristic length scale for the exponentially decaying spin-polarization in the D'yakonov-Perel' (DP) spin relaxation mechanism.¹³ However, the asymptotic values^{5,6} of the corresponding Fano factors $F_{\sigma \rightarrow \sigma'}(L \gg L_{SO}, W) > F_{\uparrow \rightarrow \uparrow}(L \gg L_{SO}, W) > 1/3$ are decreasing in narrow wires¹⁴ of width $W \ll L_{SO}$ because spin decoherence (due to entanglement of spin and orbital conducting channels¹²) and spin dephasing (due to ensemble averaging over different electrons injected through different orbital conducting channels¹²) of the DP type are suppressed greatly in such transversely confined structures.^{12,13,14}

The analysis of the spin-dependent shot noise requires to evaluate correlations between spin-resolved charge currents I^{\uparrow} and I^{\downarrow} due to the flow of spin- \uparrow and spin- \downarrow electrons through the terminals of a nanostructure¹⁵

$$S_{\alpha\beta}^{\sigma\sigma'}(t - t') = \frac{1}{2} \langle \delta\hat{I}_{\alpha}^{\sigma}(t) \delta\hat{I}_{\beta}^{\sigma'}(t') + \delta\hat{I}_{\beta}^{\sigma'}(t') \delta\hat{I}_{\alpha}^{\sigma}(t) \rangle. \quad (2)$$

Here $\hat{I}_{\alpha}^{\sigma}(t)$ is the quantum-mechanical operator of the spin-resolved ($\sigma = \uparrow, \downarrow$) charge current in lead α , $\delta\hat{I}_{\alpha}(t) = \hat{I}_{\alpha}(t) - \langle \hat{I}_{\alpha}(t) \rangle$, and $\langle \dots \rangle$ stands for both quantum-mechanical and statistical averaging over the states in the macroscopic reservoirs to which a mesoscopic conductor is attached via semi-infinite interaction-free leads. The spin-resolved noise power between terminals α and β is (conventionally defined¹ as twice) the Fourier transform of Eq. (2), $S_{\alpha\beta}^{\sigma\sigma'}(\omega) = \int d(t - t') e^{-i\omega(t-t')} S_{\alpha\beta}^{\sigma\sigma'}(t - t')$. The noise power of the total charge current $I_{\alpha} = I_{\alpha}^{\uparrow} + I_{\alpha}^{\downarrow}$ is then given by $S_{\alpha\beta}(\omega) = S_{\alpha\beta}^{\uparrow\uparrow}(\omega) + S_{\alpha\beta}^{\downarrow\downarrow}(\omega) + S_{\alpha\beta}^{\uparrow\downarrow}(\omega) + S_{\alpha\beta}^{\downarrow\uparrow}(\omega)$.

The scattering theory of quantum transport gives for the operator of *spin-resolved* charge current of spin- σ electrons flowing through terminal α

$$\hat{I}_\alpha^\sigma(t) = \frac{e}{h} \sum_{n=1}^M \iint dE dE' e^{i(E-E')t/\hbar} [\hat{a}_{\alpha n}^{\sigma\dagger}(E) \hat{a}_{\alpha n}^\sigma(E') - \hat{b}_{\beta n}^{\sigma\dagger}(E) \hat{b}_{\beta n}^\sigma(E')] \quad (3)$$

where the operator $\hat{a}_{\alpha n}^{\sigma\dagger}(E)$ [$\hat{a}_{\alpha n}^\sigma(E)$] creates [annihilates] incoming electrons in lead α which have energy E , spin- σ , and orbital part of their wave function is the transverse propagating mode n . Similarly, $\hat{b}_{\alpha n}^{\sigma\dagger}$, $\hat{b}_{\alpha n}^\sigma$ denote spin- σ electrons in the outgoing states. Using this expression in Eq. (2), and taking its Fourier transform, yields the following spin-resolved noise power spectrum formula

$$S_{\alpha\beta}^{\sigma\sigma'}(\omega) = \frac{e^2}{h} \int dE \sum_{\gamma, \gamma'} \sum_{\rho, \rho'=\uparrow, \downarrow} \text{Tr} \left[\mathbf{A}_{\gamma\gamma'}^{\rho\rho'}(\alpha, \sigma, E, E + \hbar\omega) \mathbf{A}_{\gamma'\gamma}^{\rho'\rho}(\beta, \sigma', E + \hbar\omega, E) \right] \times \{f_\gamma^\rho(E)[1 - f_{\gamma'}^{\rho'}(E + \hbar\omega)] + f_{\gamma'}^{\rho'}(E + \hbar\omega)[1 - f_\gamma^\rho(E)]\}, \quad (4)$$

where $f_\gamma^\rho(E)$ is the Fermi function in lead γ kept at temperature T_γ and spin-dependent chemical potential μ_γ^ρ of spin- ρ electrons ($\rho = \uparrow, \downarrow$). The Büttiker's current matrix¹¹ $\mathbf{A}_{\beta\gamma}^{\rho\rho'}(\alpha, \sigma, E, E')$, whose elements are

$$[\mathbf{A}_{\beta\gamma}^{\rho\rho'}(\alpha, \sigma, E, E')]_{mn} = \delta_{mn} \delta_{\beta\alpha} \delta_{\gamma\alpha} \delta^{\sigma\rho} \delta^{\sigma\rho'} - \sum_k [\mathbf{s}_{\alpha\beta}^{\sigma\rho\dagger}(E)]_{mk} [\mathbf{s}_{\alpha\gamma}^{\sigma\rho'}(E')]_{kn}, \quad (5)$$

is now generalized to include explicitly spin degrees of freedom through the spin-resolved scattering matrix connecting operators $\hat{a}_{\alpha n}^\sigma(E)$ and $\hat{b}_{\alpha n}^\sigma(E)$ via $\hat{b}_{\alpha n}^\sigma(E) = \sum_{\beta m} [\mathbf{s}_{\alpha\beta}^{\sigma\sigma'}]_{nm}(E) \hat{a}_{\beta m}^{\sigma'}(E)$. We focus on the zero-temperature limit, where the thermal (Johnson-Nyquist) contribution to the noise vanishes and the Fermi function becomes a step function $f_\alpha^\rho(E) = \theta(E - \mu_\alpha^\rho)$. Evaluation of Eq. (4) for the zero-frequency limit, $S_{\alpha\beta}^{\sigma\sigma'} \equiv S_{\alpha\beta}^{\sigma\sigma'}(\omega = 0)$, in the left lead $\alpha = 2 = \beta$ of a two-terminal mesoscopic device yields our principal result—the scattering theory formula for the shot noise arising in the course of propagation of spin-polarized current through a region with spin-dependent interactions:

$$S_{22}^{\uparrow\uparrow} = \frac{2e^2}{h} \left[\text{Tr} \left(\mathbf{t}_{21}^{\uparrow\uparrow} \mathbf{t}_{21}^{\uparrow\uparrow\dagger} \right) eV + \text{Tr} \left(\mathbf{t}_{21}^{\uparrow\downarrow} \mathbf{t}_{21}^{\uparrow\downarrow\dagger} \right) \frac{1 - |\mathbf{P}|}{1 + |\mathbf{P}|} eV - \text{Tr} \left(\mathbf{t}_{21}^{\downarrow\uparrow} \mathbf{t}_{21}^{\downarrow\uparrow\dagger} \mathbf{t}_{21}^{\uparrow\downarrow} \mathbf{t}_{21}^{\uparrow\downarrow\dagger} \right) \frac{1 - |\mathbf{P}|}{1 + |\mathbf{P}|} eV - \text{Tr} \left(\mathbf{t}_{21}^{\uparrow\uparrow} \mathbf{t}_{21}^{\uparrow\uparrow\dagger} \mathbf{t}_{21}^{\uparrow\downarrow} \mathbf{t}_{21}^{\uparrow\downarrow\dagger} \right) eV - 2 \text{Tr} \left(\mathbf{t}_{21}^{\uparrow\downarrow} \mathbf{t}_{21}^{\uparrow\downarrow\dagger} \mathbf{t}_{21}^{\uparrow\uparrow} \mathbf{t}_{21}^{\uparrow\uparrow\dagger} \right) \frac{1 - |\mathbf{P}|}{1 + |\mathbf{P}|} eV \right], \quad (6a)$$

$$S_{22}^{\downarrow\downarrow} = \frac{2e^2}{h} \left[\text{Tr} \left(\mathbf{t}_{21}^{\downarrow\downarrow} \mathbf{t}_{21}^{\downarrow\downarrow\dagger} \right) \frac{1 - |\mathbf{P}|}{1 + |\mathbf{P}|} eV + \text{Tr} \left(\mathbf{t}_{21}^{\downarrow\uparrow} \mathbf{t}_{21}^{\downarrow\uparrow\dagger} \right) eV - \text{Tr} \left(\mathbf{t}_{21}^{\downarrow\downarrow} \mathbf{t}_{21}^{\downarrow\downarrow\dagger} \mathbf{t}_{21}^{\downarrow\uparrow} \mathbf{t}_{21}^{\downarrow\uparrow\dagger} \right) \frac{1 - |\mathbf{P}|}{1 + |\mathbf{P}|} eV - \text{Tr} \left(\mathbf{t}_{21}^{\downarrow\uparrow} \mathbf{t}_{21}^{\downarrow\uparrow\dagger} \mathbf{t}_{21}^{\downarrow\downarrow} \mathbf{t}_{21}^{\downarrow\downarrow\dagger} \right) eV - 2 \text{Tr} \left(\mathbf{t}_{21}^{\downarrow\uparrow} \mathbf{t}_{21}^{\downarrow\uparrow\dagger} \mathbf{t}_{21}^{\downarrow\downarrow} \mathbf{t}_{21}^{\downarrow\downarrow\dagger} \right) \frac{1 - |\mathbf{P}|}{1 + |\mathbf{P}|} eV \right], \quad (6b)$$

$$S_{22}^{\uparrow\downarrow} = -\frac{2e^2}{h} \left[\text{Tr} \left(\mathbf{t}_{21}^{\uparrow\downarrow} \mathbf{t}_{21}^{\uparrow\uparrow\dagger} \mathbf{t}_{21}^{\uparrow\downarrow} \mathbf{t}_{21}^{\uparrow\downarrow\dagger} \right) \frac{1 - |\mathbf{P}|}{1 + |\mathbf{P}|} eV + \text{Tr} \left(\mathbf{t}_{21}^{\downarrow\uparrow} \mathbf{t}_{21}^{\downarrow\uparrow\dagger} \mathbf{t}_{21}^{\uparrow\downarrow} \mathbf{t}_{21}^{\uparrow\downarrow\dagger} \right) eV + \text{Tr} \left(\mathbf{t}_{21}^{\downarrow\downarrow} \mathbf{t}_{21}^{\downarrow\downarrow\dagger} \mathbf{t}_{21}^{\uparrow\uparrow} \mathbf{t}_{21}^{\uparrow\uparrow\dagger} \right) \frac{1 - |\mathbf{P}|}{1 + |\mathbf{P}|} eV + \text{Tr} \left(\mathbf{t}_{21}^{\downarrow\uparrow} \mathbf{t}_{21}^{\downarrow\uparrow\dagger} \mathbf{t}_{21}^{\downarrow\downarrow} \mathbf{t}_{21}^{\downarrow\downarrow\dagger} \right) \frac{1 - |\mathbf{P}|}{1 + |\mathbf{P}|} eV \right], \quad (6c)$$

$$S_{22}^{\downarrow\uparrow} = -\frac{2e^2}{h} \left[\text{Tr} \left(\mathbf{t}_{21}^{\uparrow\uparrow} \mathbf{t}_{21}^{\uparrow\uparrow\dagger} \mathbf{t}_{21}^{\downarrow\downarrow} \mathbf{t}_{21}^{\downarrow\downarrow\dagger} \right) \frac{1 - |\mathbf{P}|}{1 + |\mathbf{P}|} eV + \text{Tr} \left(\mathbf{t}_{21}^{\uparrow\downarrow} \mathbf{t}_{21}^{\uparrow\downarrow\dagger} \mathbf{t}_{21}^{\downarrow\uparrow} \mathbf{t}_{21}^{\downarrow\uparrow\dagger} \right) eV + \text{Tr} \left(\mathbf{t}_{21}^{\downarrow\uparrow} \mathbf{t}_{21}^{\downarrow\uparrow\dagger} \mathbf{t}_{21}^{\downarrow\downarrow} \mathbf{t}_{21}^{\downarrow\downarrow\dagger} \right) \frac{1 - |\mathbf{P}|}{1 + |\mathbf{P}|} eV + \text{Tr} \left(\mathbf{t}_{21}^{\downarrow\downarrow} \mathbf{t}_{21}^{\downarrow\downarrow\dagger} \mathbf{t}_{21}^{\uparrow\uparrow} \mathbf{t}_{21}^{\uparrow\uparrow\dagger} \right) \frac{1 - |\mathbf{P}|}{1 + |\mathbf{P}|} eV \right]. \quad (6d)$$

Here the elements of the transmission matrix $\mathbf{t}_{21}^{\sigma\sigma'}$, which is a block of the full scattering matrix, determine the probability $|[\mathbf{t}_{21}^{\sigma\sigma'}]_{nm}|^2$ for spin- σ' electron incident in lead 1 in the orbital conducting channel m to be transmitted to lead 2 as spin- σ electron in channel n . The direction of the spin-polarization vector of injected electrons

selects the spin-quantization axis for \uparrow, \downarrow , while its magnitude quantifies the degree of spin polarization which was introduced into Eq. (4) via spin-dependent chemical potentials in the injecting (left) lead,⁹ $\mu_1^\uparrow = E_F + eV$ and $\mu_1^\downarrow = E_F + eV(1 - |\mathbf{P}|)/(1 + |\mathbf{P}|)$. In the collecting (right)

lead the chemical potentials for both spin-species are the same $\mu_1^\uparrow = \mu_2^\downarrow = E_F$, where E_F is the Fermi energy. For instance, injection of fully spin- \uparrow polarized current $|\mathbf{P}| = 1$ from the left lead (e.g., made of half-metallic ferromagnet) means that there is no voltage drop for spin- \downarrow electrons $\mu_1^\downarrow = \mu_2^\downarrow = E_F$, so that they do not contribute to transport.

Equations (6), together with the expressions for average spin-resolved currents collected in the right lead,

$$I_2^\uparrow \equiv \langle \hat{I}_2^\uparrow(t) \rangle = \left(G_{21}^{\uparrow\uparrow} + G_{21}^{\uparrow\downarrow} \frac{1 - |\mathbf{P}|}{1 + |\mathbf{P}|} \right) V \quad (7a)$$

$$I_2^\downarrow \equiv \langle \hat{I}_2^\downarrow(t) \rangle = \left(G_{21}^{\downarrow\uparrow} + G_{21}^{\downarrow\downarrow} \frac{1 - |\mathbf{P}|}{1 + |\mathbf{P}|} \right) V \quad (7b)$$

allow us to obtain in Fig. 1 the Fano factors of parallel and antiparallel spin valve setups, $F_{\uparrow\rightarrow\uparrow} = S_{22}^{\uparrow\uparrow}(|\mathbf{P}| = 1)/[2eI_2^\uparrow(|\mathbf{P}| = 1)]$ and $F_{\uparrow\rightarrow\downarrow} = S_{22}^{\downarrow\downarrow}(|\mathbf{P}| = 1)/[2eI_2^\downarrow(|\mathbf{P}| = 1)]$, as well as $F_{\uparrow\rightarrow\uparrow\downarrow} = S_{22}(|\mathbf{P}| = 1)/[2eI_2(|\mathbf{P}| = 1)]$ for ferromagnet/Rashba-wire/paramagnet configuration where the sum of both spin-resolved currents is collected in the right paramagnetic lead $I_2 = I_2^\uparrow + I_2^\downarrow$. Here the spin-resolved conductances are given by the Landauer-type formula $G_{21}^{\sigma\sigma'} = \frac{e^2}{h} \sum_{n,m=1}^M |[\mathbf{t}_{21}^{\sigma\sigma'}]_{nm}|^2$. The consequences of the scattering theory expressions, Eq. (6) and Eq. (7), can be worked out either by analytical means (such as the random matrix theory⁶ or matching the wave function across single- or two-channel structures⁹) or by numerically exact real \otimes spin space Green functions¹² employed here to take as an input the microscopic Hamiltonian Eq. (1) of *multichannel* nanostructures.

For very small SO coupling and, therefore, large $L_{SO} \rightarrow \infty$, the Fano factors $F_{\uparrow\rightarrow\uparrow}$ and $F_{\uparrow\rightarrow\uparrow\downarrow}$ start from the universal value $F = 1/3$ for unpolarized electrons in diffusive wires, and then increase toward their asymptotic values,¹⁶ $F_{\uparrow\rightarrow\uparrow}(L \gg L_{SO}) \approx F_{\uparrow\rightarrow\downarrow}(L \gg L_{SO}) \simeq 0.7$ and $F_{\uparrow\rightarrow\uparrow\downarrow}(L \gg L_{SO}) \simeq 0.55$. Such substantial enhancement of the spin-dependent shot noise is due to spin decoherence and dephasing processes in SO coupled structures that are reducing the off-diagonal elements of the current spin-density matrix,¹² which initially describes pure injected spin states $\hat{\rho}_c^2 = \hat{\rho}_c$ from the left lead. However, these asymptotic Fano factor values are lowered in narrow wires where transverse confinement slows down the DP spin relaxation in the picture of semiclassical diffusion,¹³ or reduces the size of the “environment” of orbital conducting channels (i.e., their number) to which the spin can entangle in fully quantum transport picture.¹² These effects, essential for the development of

all-electrical spintronic devices, have been confirmed in recent experiments.¹⁴ Thus, in such structures spin coherence, measured by the Bloch vector $|\mathbf{P}_{\text{detect}}|$ extracted from the current spin-density matrix¹² in the right lead

$$\hat{\rho}_c^\uparrow = \frac{e^2/h}{G_{21}^{\uparrow\uparrow} + G_{21}^{\uparrow\downarrow}} \sum_{n,m=1}^M \begin{pmatrix} |[\mathbf{t}_{21}^{\uparrow\uparrow}]_{nm}|^2 & |[\mathbf{t}_{21}^{\uparrow\uparrow}]_{nm} [\mathbf{t}_{21}^{\downarrow\uparrow}]_{nm}^*| \\ |[\mathbf{t}_{21}^{\uparrow\uparrow}]_{nm}^* [\mathbf{t}_{21}^{\downarrow\uparrow}]_{nm}| & |[\mathbf{t}_{21}^{\downarrow\uparrow}]_{nm}|^2 \end{pmatrix}, \quad (8)$$

remains close to one for $L \lesssim L_{SO}$, as demonstrated in Fig. 1(c). The preservation of quantum coherence also allows for spin-interference signatures to become visible in the shot noise of Fig. 1(a) as Rabi oscillations of the Fano factor between $F_{\sigma\rightarrow\sigma'} = 1/3$ and $F_{\sigma\rightarrow\sigma'} = 1$ on the L_{SO} -scale. The shot noise in the antiparallel configuration reaches the full Poissonian value $F_{\uparrow\rightarrow\downarrow}(L \ll L_{SO}) \simeq 1$ in the limit of small SO coupling since the probability that the spin state which has huge overlap with $|\uparrow\rangle$ can enter into the right electrode with empty spin- \uparrow states is minuscule, which leads to the tunneling-type^{1,5} of shot noise where electrons propagate independently (i.e., without being correlated by the Fermi statistics). In the asymptotic limit $L \gg L_{SO}$, injected spins loose their memory on a very short length scale so that $F_{\uparrow\rightarrow\downarrow}$ acquires the same value as the other two Fano factors discussed above.

In conclusion, we have derived a scattering theory formula for the charge and spin shot noise which takes as an input the degree of quantum coherence of injected spins, i.e., the corresponding polarization of charge current they comprise. The application of this formalism to two-terminal multichannel diffusive quantum wires with the Rashba SO coupling unveils how spin-decoherence and spin-dephasing processes, rather than just generic “spin-flipping”,⁵ are essential for the dramatic enhancement of the shot noise of charge current in spin-dependent transport.^{5,6} That is, in narrow wires where the loss of spin coherence is suppressed and $|\mathbf{P}_{\text{detect}}|$ decays much slower [Fig. 1(c)] than in bulk systems, the enhancement of the Fano factor (above $F = 1/3$ of spin-degenerate diffusive transport¹) in the strong SO coupling regime $L \gg L_{SO}$ (inducing fast spin dynamics within the wire) is reduced even though the *partially coherent* $0 < |\mathbf{P}_{\text{detect}}| < 1$ spin state continues to “flip”, but through (partially coherent¹²) spin precession.

Acknowledgments

This study was supported in part by the University of Delaware Research Foundation.

¹ Ya. M. Blanter and M. Büttiker, Phys. Rep. **322**, 1 (2000).

² H. Schomerus and P. Jacquod, J. Phys. A: Math. Gen. **38**, 10663 (2005).

³ A. H. Steinbach, J. M. Martinis, and M. H. Devoret, Phys.

Rev. Lett. **76**, 3806 (1996).

⁴ Y. Tserkovnyak and A. Brataas, Phys. Rev. B **64**, 214402 (2001).

⁵ E. G. Mishchenko, Phys. Rev. B **68**, 100409(R) (2003).

⁶ A. Lamacraft, Phys. Rev. B **69**, 081301(R) (2004).

⁷ K. E. Nagaev and L. I. Glazman, Phys. Rev. B **73**, 054423 (2006).

⁸ W. Belzig and M. Zareyan, Phys. Rev. B **69**, 140407(R) (2004).

⁹ J. C. Egues *et al.*, Phys. Rev. B **72**, 235326 (2005).

¹⁰ R. Winkler, *Spin-Orbit Coupling Effects in Two-Dimensional Electron and Hole Systems* (Springer, Berlin, 2003).

¹¹ M. Büttiker, Phys. Rev. B **46**, 12485 (1992).

¹² B. K. Nikolić and S. Souma, Phys. Rev. B **71**, 195328 (2005).

¹³ A. G. Mal'shukov and K. A. Chao, Phys. Rev. B **61**, R2413 (2000); A. A. Kiselev and K. W. Kim, Phys. Rev. B **61**, 13115 (2000).

¹⁴ A. W. Holleitner *et al.*, cond-mat/0602155.

¹⁵ O. Sauret and D. Feinberg, Phys. Rev. Lett. **92**, 106601 (2004).

¹⁶ Note that phenomenological model of Ref. 6, characterized by spin-relaxation length L_s , finds $F_{\uparrow\rightarrow\uparrow\downarrow}(L \gg L_s) = 2/3$.